

Supporting Information

Identifying the roles of imine and alkyne linkages in Photocatalytic Hydrogen Evolution over Thiadiazole-Based Covalent Organic Frameworks

Lei Hao,^{a+} Kaihui Huang,^{a+} Ningxin Wang,^{b+} Rongchen Shen,^a Shuling Chen,^a Weiling Bi,^a Neng Li,^{c*} Peng zhang,^d Youji Li^e and Xin Li^{a*}

[a] Institute of Biomass Engineering, Key Laboratory of Energy Plants Resource and Utilization, Ministry of Agriculture and Rural Affairs, South China Agricultural University, Guangzhou 510642, China

E-mail: Xinli@scau.edu.cn

[b] College of Materials and Energy, South China Agricultural University, Guangdong, Guangzhou 510642, PR China

[c] State Key Laboratory of Silicate Materials for Architectures, Wuhan University of Technology, Hubei, 430070, China E-mail: lineng@whut.edu.cn

E-mail: lineng@whut.edu.cn

[d] State Centre for International Cooperation on Designer Low-Carbon & Environmental Materials (CDLCEM), School of Materials Science and Engineering, Zhengzhou University, Henan, Zhengzhou, 450001, P. R. China

[e] College of Chemistry and Chemical Engineering, Jishou University, Jishou 416000, Hunan, China

[+] These authors contributed equally to this work

Materials and Characterization

All reagents and solvents were used as received from commercial sources, 4,4',4''-(1,3,5-triazine-2,4,6-triyl)trianiline, 4,7- dibromobenzo[c][1,2,5] thiadiazole and Acetic acid were purchased from Macklin industrial corporation, 4-(4,4,5,5-tetramethyl-1,3,2-dioxaborolan-2-yl)benzaldehyde, 2-(4-bromophenyl)-4,4,5,5-tetramethyl-1,3,2-dioxaborolane and ethynyltrimethylsilane from Yanshen industrial corporation.

General Characterization:

The FT-IR spectra were performed on a Bruker ALPHA spectrometer in the frequency range of 400-4000 cm^{-1} . The ^{13}C CP/MAS NMR spectra were recorded with the contact time of 2 ms (ramp 100) and a pulse delay of 3 s with a 4-mm double resonance probe. Fluorescence spectra were performed on a Hitachi F-7000 fluorescence spectrophotometer at 25 °C. Thermogravimetric analysis (TGA) of all Te-COFs were evaluated using a NETZSCH TG 5500 analyzer over the temperature range from room temperature to 800 °C under N_2 atmosphere with a heating rate of 10 °C/min. The Powder X-ray diffraction (PXRD) patterns were recorded on X-ray diffractometer RIGAKU SMARTLAB9KW (unless noted in caption) or DX-27mini X-Ray diffractometer with a Cu-target tube and a graphite monochromator. Transmission electron microscopes (TEM) and high-resolution transmission electron microscopies (HR-TEM) were performed on a JEOL model JSM-2100F. Field emission scanning electron microscopies (FE-SEM) were performed on a Hitachi SU8010 microscope operating at an accelerating voltage of 5.0 kV. Surface areas and pore size distributions were measured by nitrogen adsorption and desorption using a Bel Japan Inc. model BELSOPR-mini II analyser and the samples were activated at 120 °C for 3 h under vacuum (10^{-5} bar) before analysis. The pore size distribution was calculated from the adsorption branch with the nonlocal density functional theory (NLDFT). Structural simulations of Te-COFs were performed in the Accelrys Materials Studio software package using the Forcite module. The structural refinements were carried out using the Pawley refinement of the Reflex module. The final lattice parameters and the refined PXRD patterns were obtained until the values of R_{wp} and R_{p} converged. Photoluminescence (PL) spectra were collected on Hitachi F-7000 fluorescence spectrophotometer. Meanwhile, time-correlated single photon counting measurements were conducted using a single photon counting controller (Fluorohub, Horiba Scientific) to collect the photoluminescence decay profiles¹.

Photocatalytic Tests:

5 mg photocatalyst suspended in 80 mL H_2O with 0.1 M ascorbic acid as the sacrificial agent was added in a Hermetic device mainly composed of a quartz tube and sealing components. Prior to the photocatalytic test, the device was purged with Ar flow to remove air. A 300 W Xe lamp (Beijing Perfectlight Technology Co., Ltd. Perfect Light PLSSXE 300) was used as the light source. A cutoff filter (Kenko L-42)

was used to achieve visiblelight irradiation ($\lambda > 420$ nm) with a power density of 100 mWcm⁻². The amount of H₂ evolved was determined using gas chromatography (SHIMADZU GC-2014, thermal conductivity detector (TCD), Ar carrier, Agilent). The photocatalytic tests were repeated for three times for each sample with relative error < 10%. Cycling photocatalytic tests were performed using the same way after the samples were collected and washed with water².

DFT calculations details:

All calculations are performed by well-defined density function theory (DFT)-based package DMol³. The work function (Φ) is a very important specification the potential barrier to emission of the electron for the structure. The work function, ϕ , of a material is an important property, commonly employed as an intrinsic reference for band alignment. It can be defined as follows (Eq. (1))⁴.

$$\phi = E_{vac} - E_f \quad (1)$$

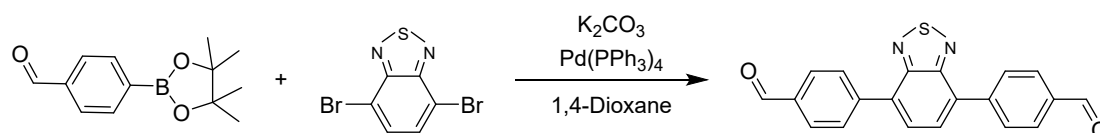
where E_{vac} is the vacuum energy of a stationary electron near the surface of the material and E_f denotes the ground state electronic structure calculation.

External quantum efficiency measurements:

The apparent quantum yield for the photocatalytic H₂ evolution was measured using $\lambda = 420$ nm (129.5 mW) and $\lambda = 490$ nm (97.1 mW) LEDs controlled by an IsoTech IPS303DD power supply. For the measurement, TeTz-COF1 or TeTz-COF2 (10 mg) was suspended in an aqueous solution containing ascorbic acid (0.1 M, 80 mL) with diluted hexachloroplatinic acid solution as a platinum precursor (4 % loading) before illuminating with the LED. The light intensity was measured with a ThorLabs S120VC photodiode power sensor controlled by a ThorLabs PM100D Power and Energy Meter Console and the apparent quantum yield was estimated using the equation below.

Synthetic Procedures

1.Synthetic of 4,4'-(benzo[c][1,2,5]thiadiazole-4,7-diyl)dibenzaldehyde

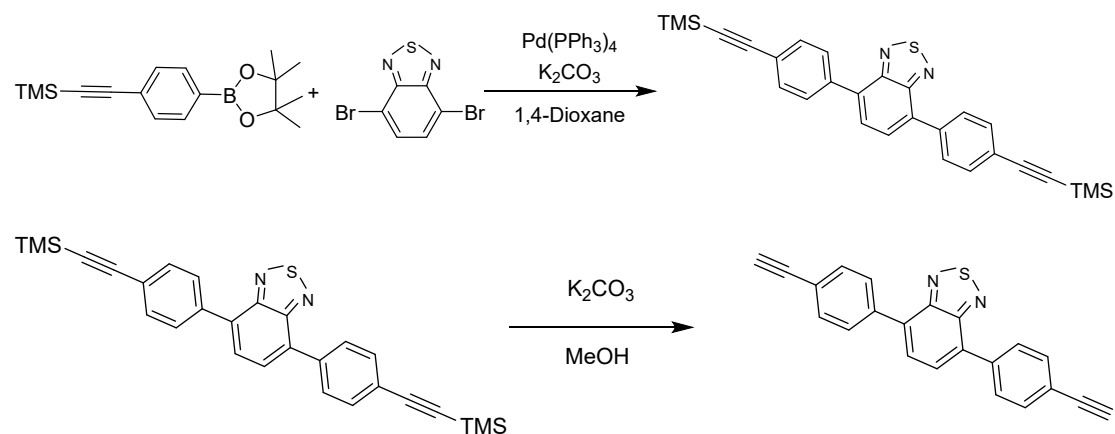


Scheme S1. The synthesis of 4,4'-(benzothiadiazole-4,7-diyl)dibenzaldehyde.

4-(4,4,5,5-tetramethyl-1,3,2-dioxaborolan-2-yl)benzaldehyde (2 mmol, 464 mg), 4,7-dibromobenzo[c][1,2,5]thiadiazole (1 mmol, 294 mg), Potassium carbonate (2.4 mmol, 553 mg), Tetrakis(triphenylphosphine)palladium(0) (0.1 mmol, 115 g), and dioxane/water (50 mL, v/v = 4/1) were placed in a Schlenk tube under N₂ atmosphere, and refluxed for 2 days. After cooling to room temperature, the mixture was filtered through celite and then concentrated and purified by chromatography to give product 275.5 mg of 4,4'-(benzo[c][1,2,5]thiadiazole-4,7-diyl)dibenzaldehyde (80% yield). ¹H NMR (400 MHz, CDCl₃) δ = 10.13 (s, 2H), 8.18-8.17 (m, 4H), 8.08-8.07

(m, 4H), 7.91 (s, 2H).

2.Synthetic of 4,7-bis(4-ethynylphenyl)benzo[c][1,2,5]thiadiazole

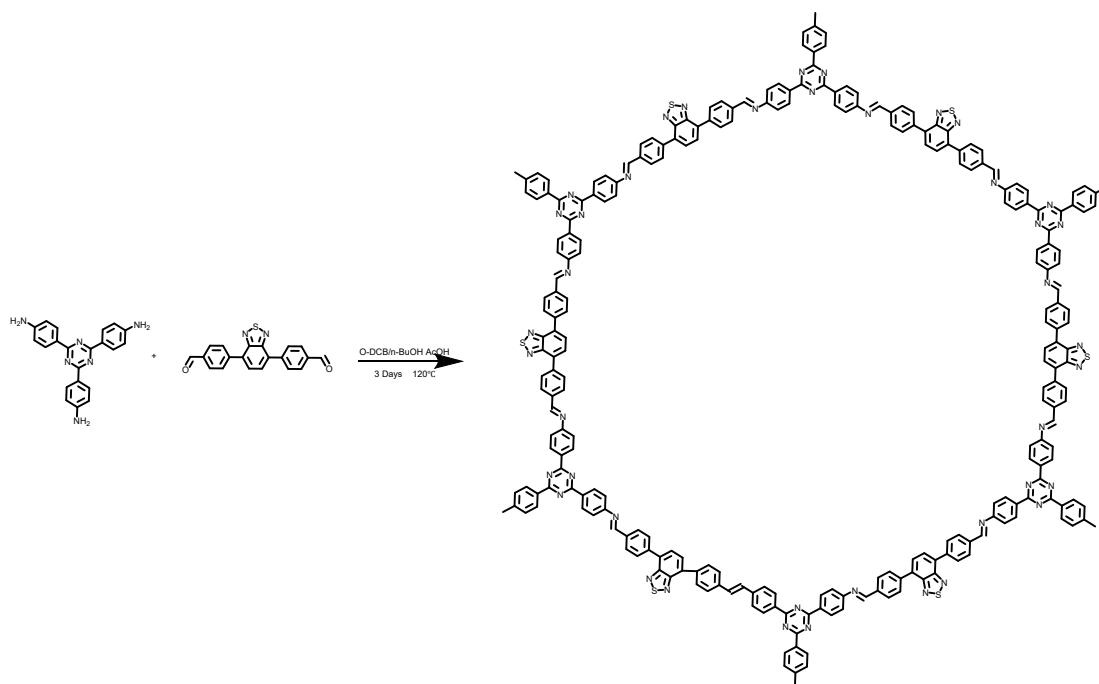


Scheme S2. The synthesis of 4,7-bis(4-ethynylphenyl)benzo[c][1,2,5]thiadiazole.

(4,5,5-trimethyl-2-(4-((trimethylsilyl)ethynyl)phenyl)-1,3,2-dioxaborolan-4-yl)methylum (2 mmol, 599 mg), 4,7-dibromobenzo[c][1,2,5]thiadiazole (1 mmol, 294 mg), Potassium carbonate (2.4 mmol, 553 mg), Tetrakis(triphenylphosphine)palladium(0) (0.1 mmol, 115 g), and dioxane (50 mL) were placed in a Schlenk tube under N₂ atmosphere, and refluxed for 2 days. After cooling to room temperature, the mixture was filtered through celite and then concentrated and purified by chromatography to give crude product, and the crude product was added to 50 ml of MeOH, then 200 mg of K₂CO₃ was added, and the mixture was stirred at room temperature for 1 h. The reaction was then extracted with water and ethyl acetate. Concentrated and purified by column chromatography. get the product 242.2mg of 4,7-

bis(4-ethynylphenyl)benzo[*c*][1,2,5]thiadiazole (72% yield). ¹H NMR (400 MHz, CDCl₃) δ = 8.07 (d, J = 8.0 Hz 4H), 8.02 (s, 2H), 7.67 (m, J = 8.0 Hz, 4H), 4.37 (s, 2H).

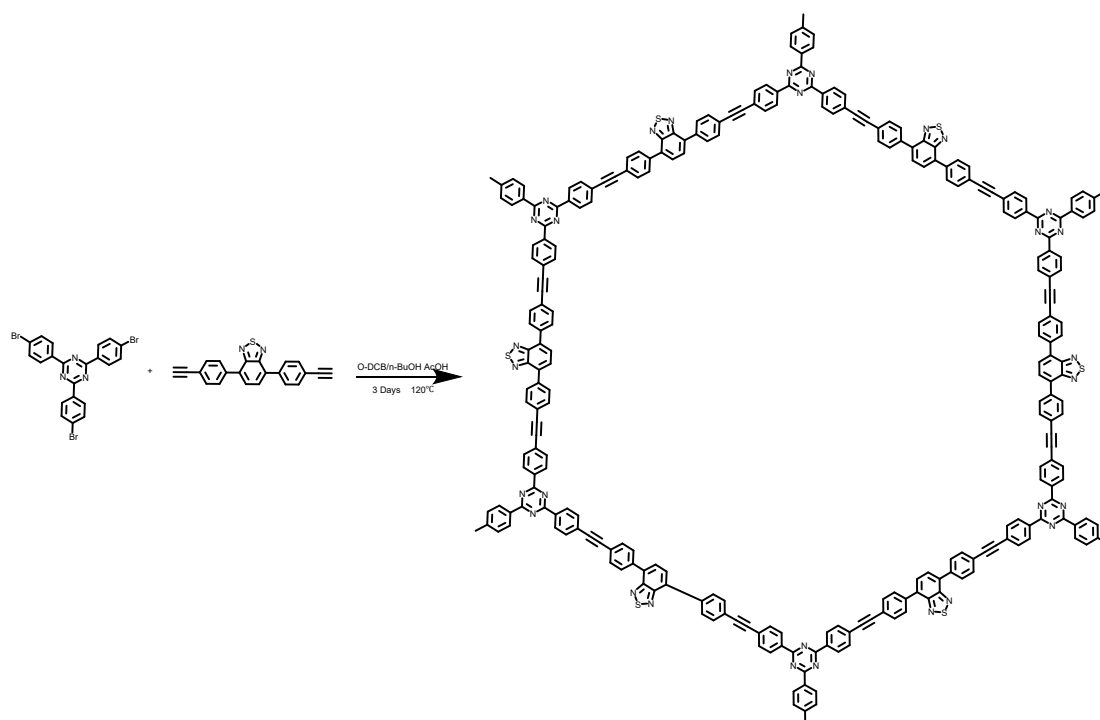
3.Synthetic of TeTz-COF1



Scheme S3. The synthesis of TeTz-COF1.

A Pyrex tube was charged with 4,4',4''-(1,3,5-triazine-2,4,6-triyl)trianiline (35.4 mg, 0.1 mmol), 4,4'-(benzo[*c*][1,2,5]thiadiazole-4,7-diyl)dibenzaldehyde (51.6 mg, 0.15 mmol), 1,2-Dichlorobenzene (0.7 mL), *n*-butanol (0.3 mL), and acetic acid (3M, 0.1 mL). This mixture was homogenized by sonication for 20 minutes and the tube was then flash frozen at 77 K (liquid N₂ bath) and degassed by three freeze-pump-thaw cycles and evacuated to an internal pressure of 100 mTorr. The tube was sealed off and then heated at 120 °C for 3 days. The dark red precipitate was collected by centrifugation and washed with *N,N*-dimethylformamide (100 mL) and anhydrous acetone (200 mL). After drying at 120 °C, the product was obtained as a deep red-colored powder (70 mg, 80%).

4.Synthetic of TeTz-COF2



Scheme S4. The synthesis of TeTz-COF2.

A Pyrex tube was charged with 2,4,6-tris(4-bromophenyl)-1,3,5-triazine (54.6 mg, 0.1 mmol), 4,7-bis(4-ethynylphenyl)benzo[c][1,2,5]thiadiazole (50.4 mg, 0.15 mmol), 1,2-Dichlorobenzene (0.7 mL), n-butanol (0.3 mL), and acetic acid (3M, 0.1 mL). This mixture was homogenized by sonication for 20 minutes and the tube was then flash frozen at 77 K (liquid N₂ bath) and degassed by three freeze-pump-thaw cycles and evacuated to an internal pressure of 100 mTorr. The tube was sealed off and then heated at 120 °C for 3 days. The dark red precipitate was collected by centrifugation and washed with N,N-dimethylformamide (100 mL) and anhydrous acetone (200 mL). After drying at 120 °C, the product was obtained as a deep red-colored powder (93.5 mg, 89%).

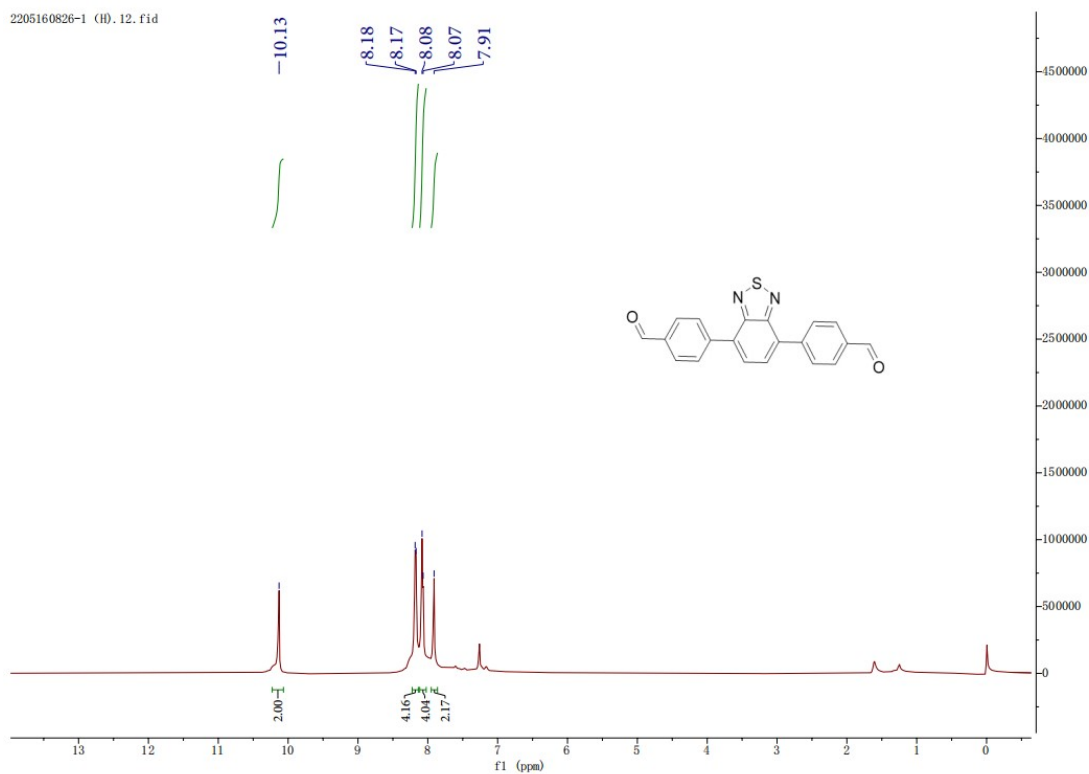


Figure S1. ^1H NMR spectrum of 4,4'-(benzo[c][1,2,5]thiadiazole-4,7-diyl)dibenzaldehyde (400 MHz, DMSO)

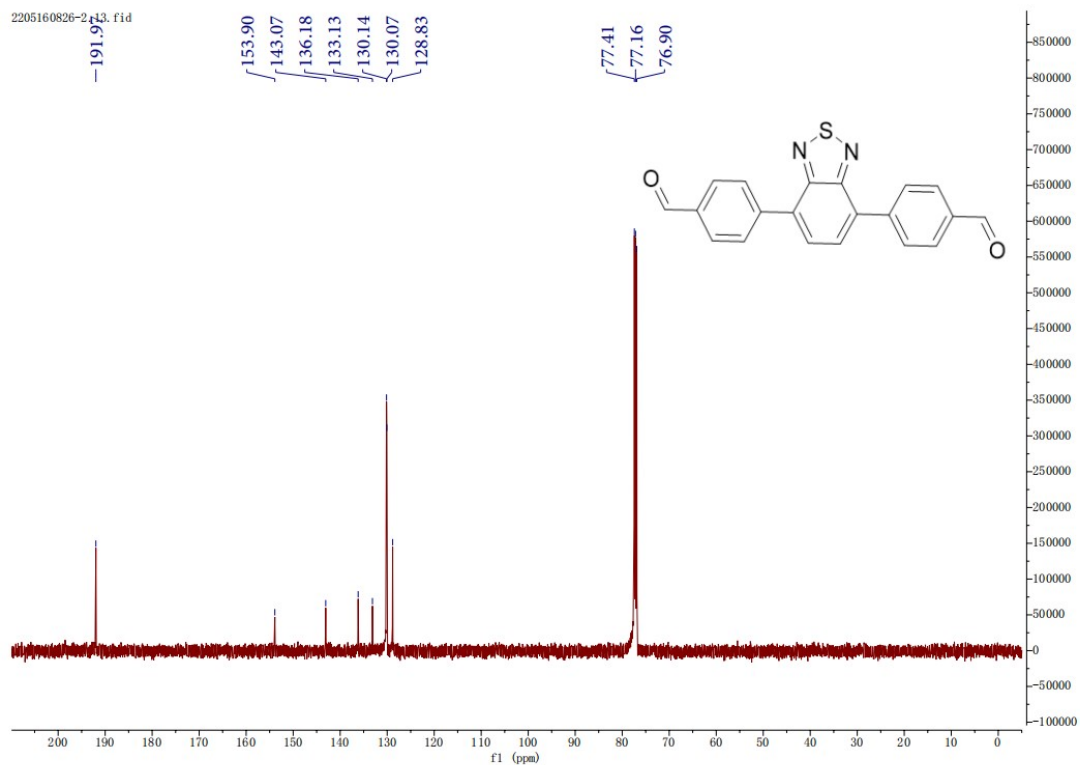


Figure S2. ^{13}C NMR spectrum of 4,4'-(benzo[c][1,2,5]thiadiazole-4,7-diyl)dibenzaldehyde (100 MHz, DMSO)

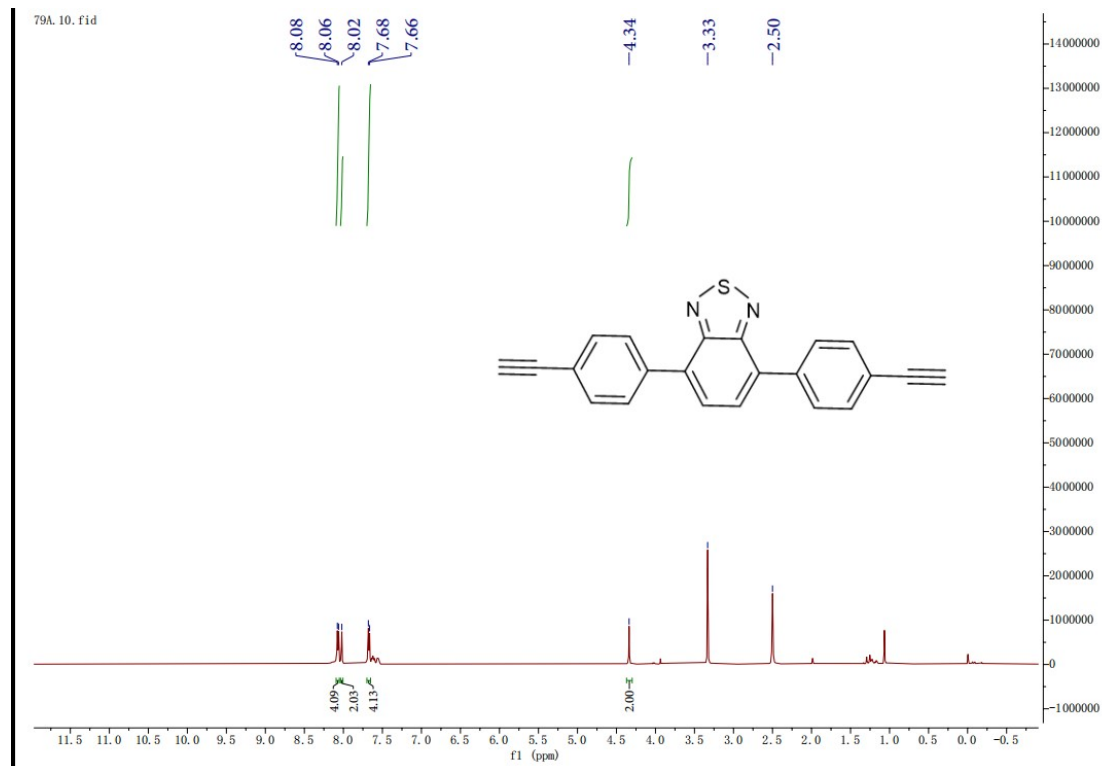


Figure S3. ^1H NMR spectrum of 4,7-bis(4-ethynylphenyl)benzo[c][1,2,5]thiadiazole (400 MHz, CDCl_3)

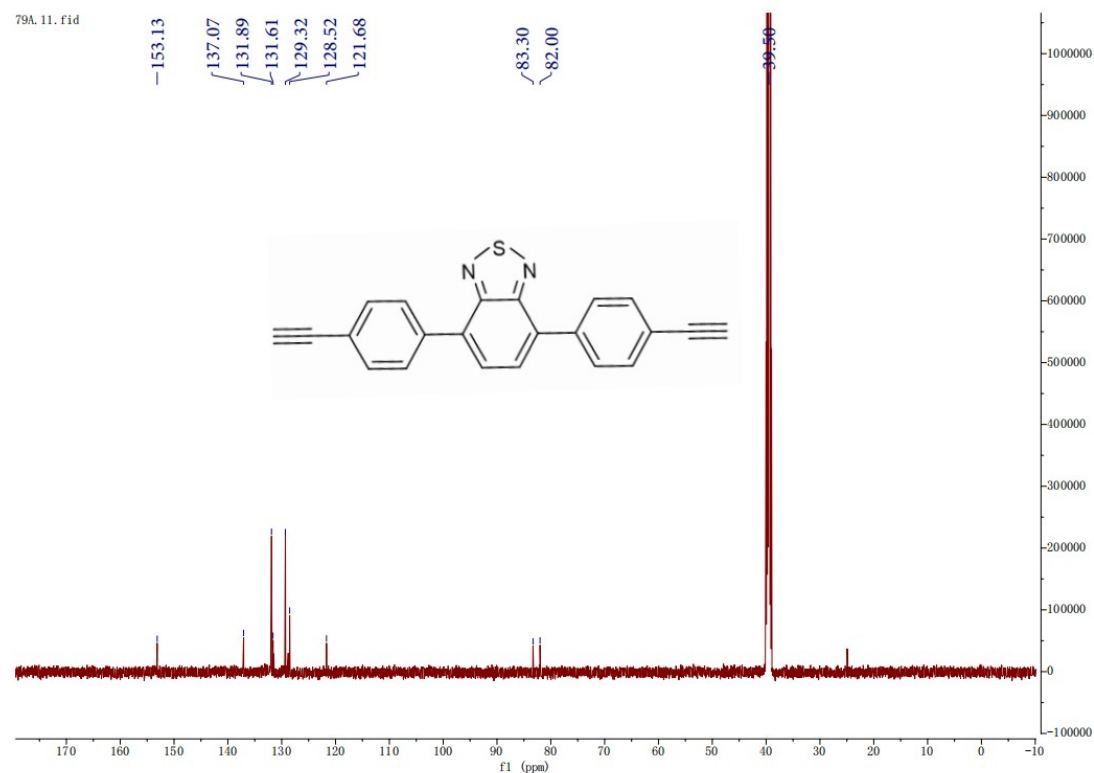


Figure S4. ^{13}C NMR spectrum of 4,7-bis(4-ethynylphenyl)benzo[c][1,2,5]thiadiazole (100 MHz, DMSO)

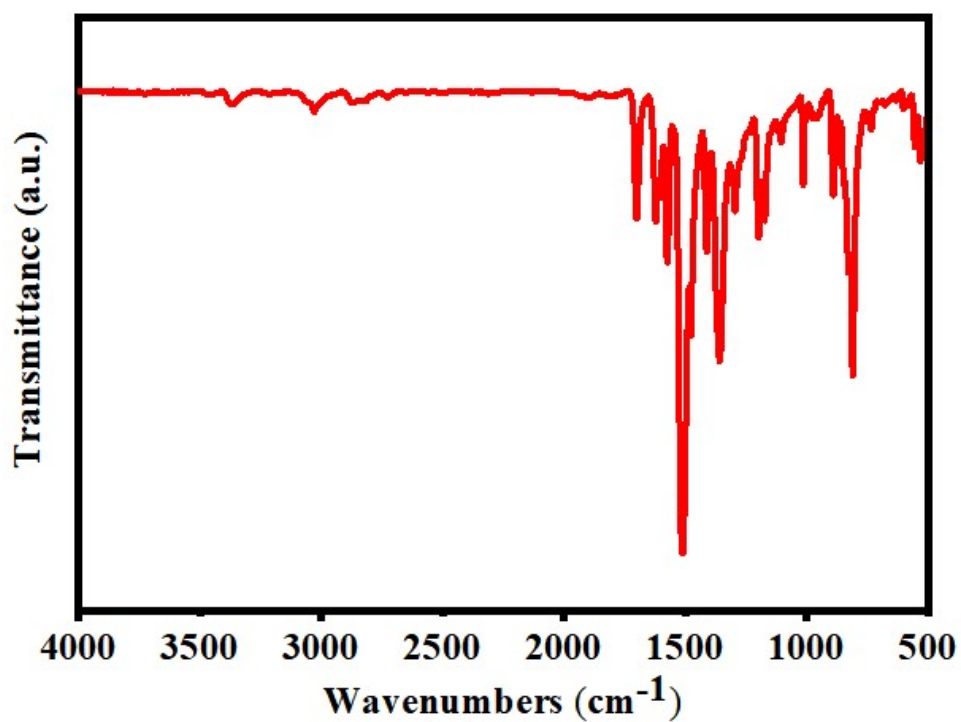


Figure S5. FT-IR spectra of TeTz-COF1

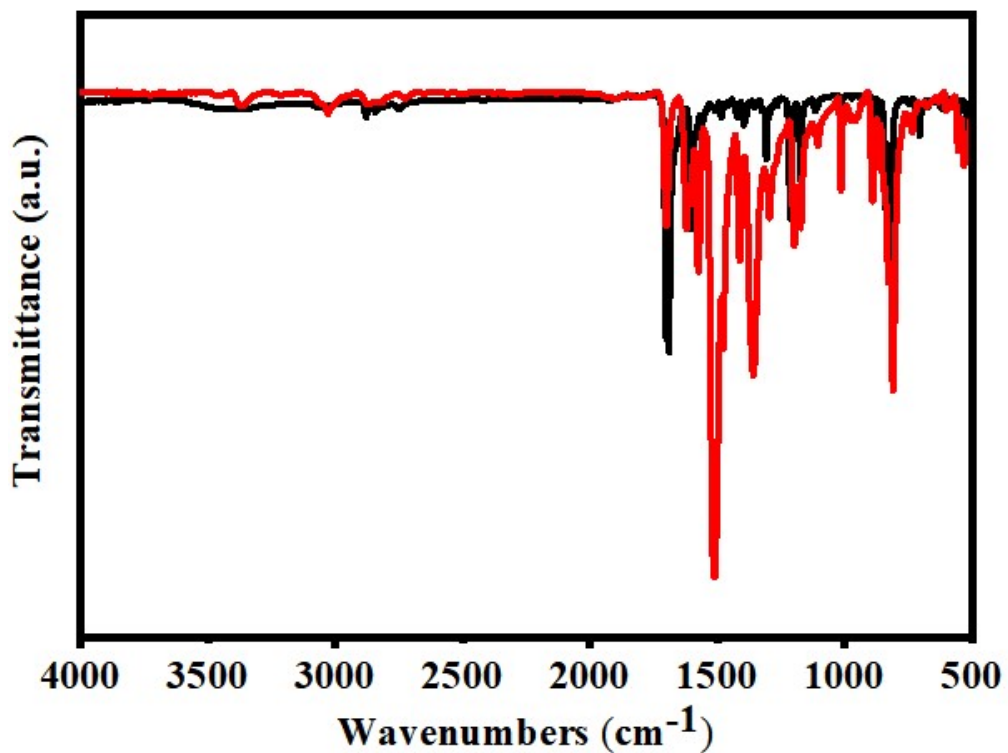


Figure S6. FT-IR spectra of TeTz-COF1 (red) and 4,4'-(benzo[c][1,2,5]thiadiazole-4,7-diyl)dibenzaldehyde (black)

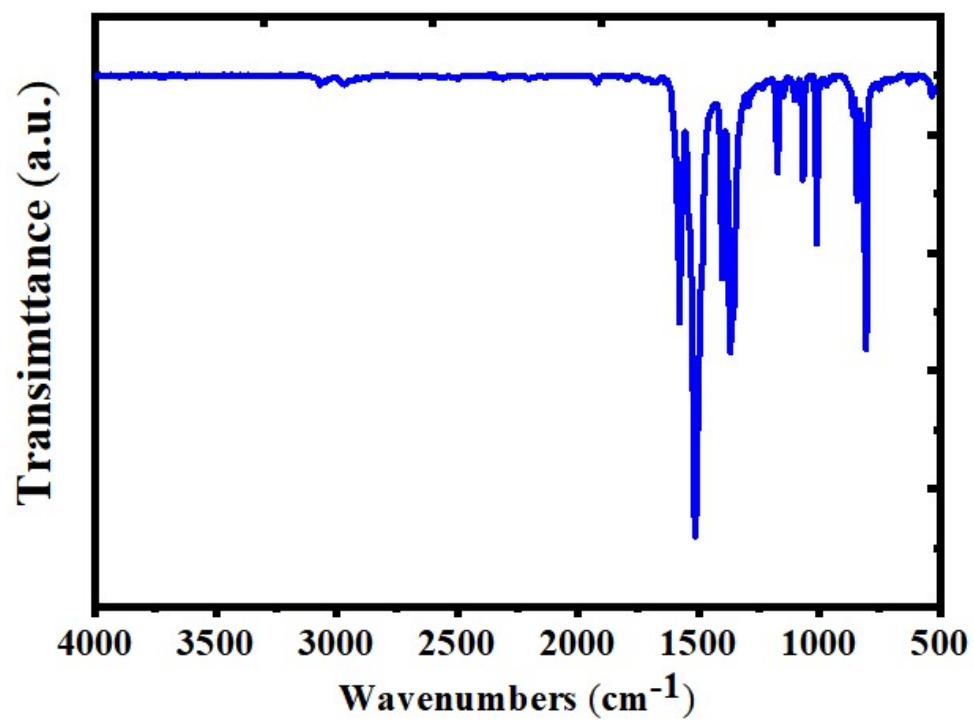


Figure S7. FT-IR spectra of TeTz-COF2

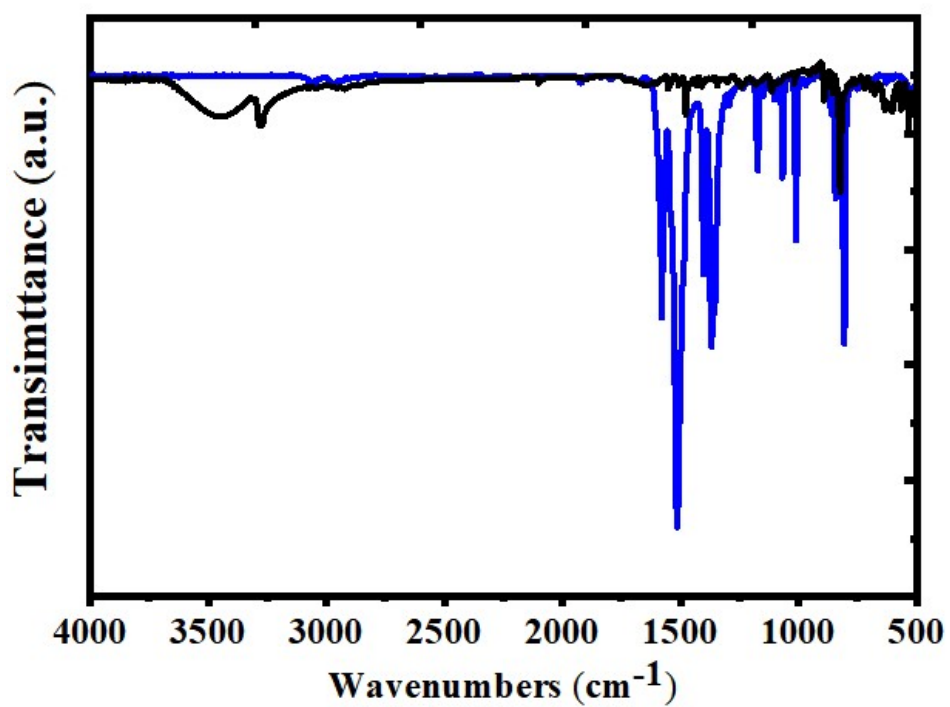


Figure S8. FT-IR spectra of TeTz-COF2 (blue) and 4,7-bis(4-ethynylphenyl)benzo[c][1,2,5]thiadiazole (black)

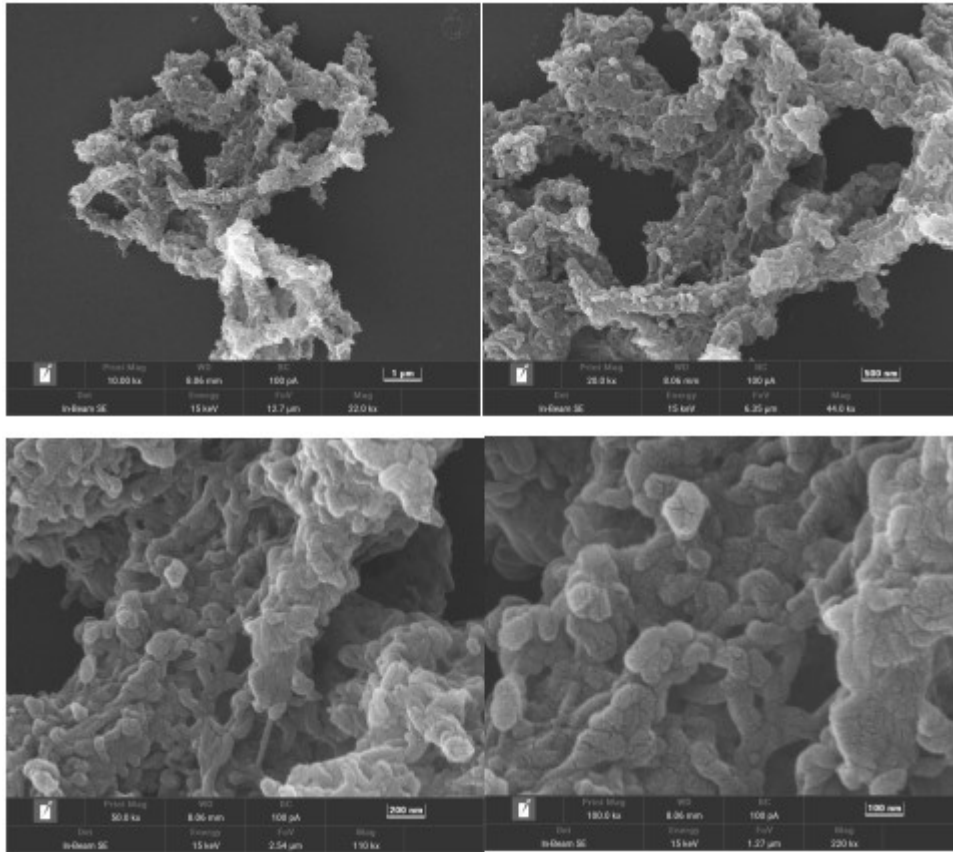


Figure S9. SEM image of TeTz-COF1

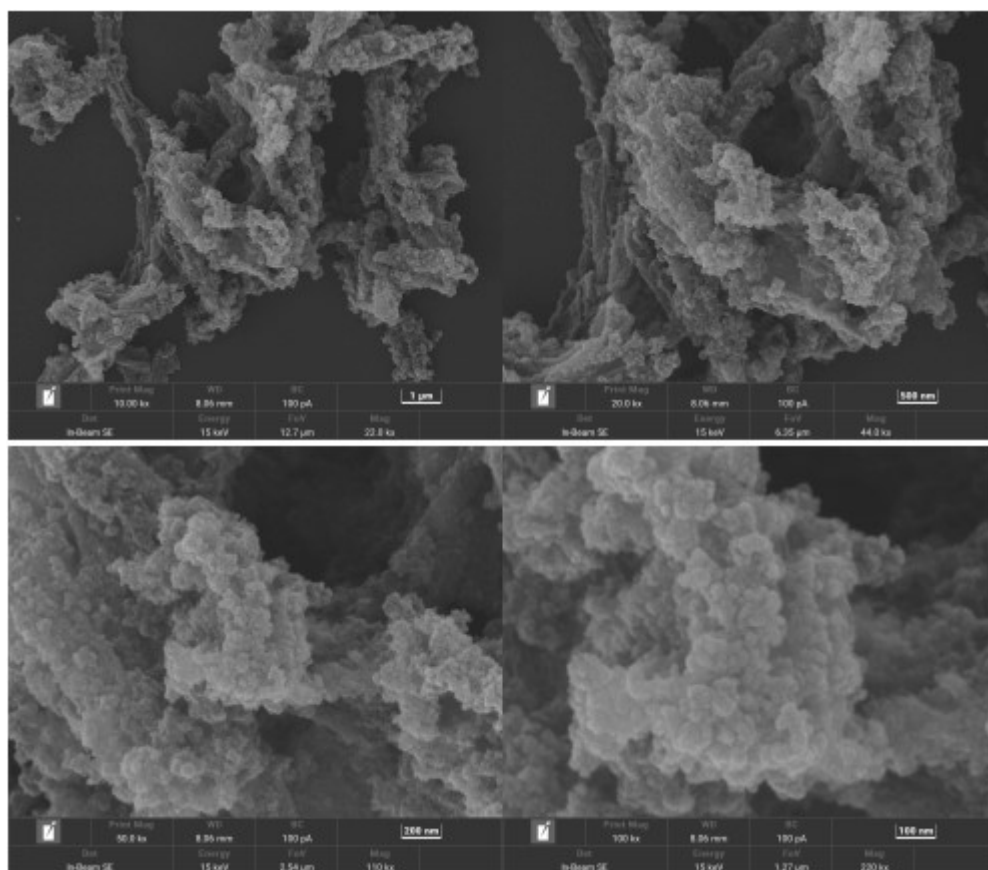


Figure S10. SEM image of TeTz-COF2

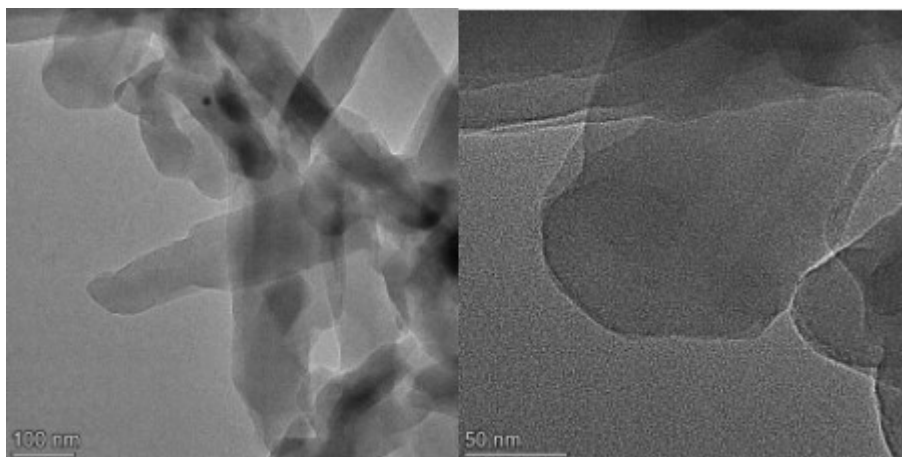


Figure S11. TEM image of TeTz-COF1

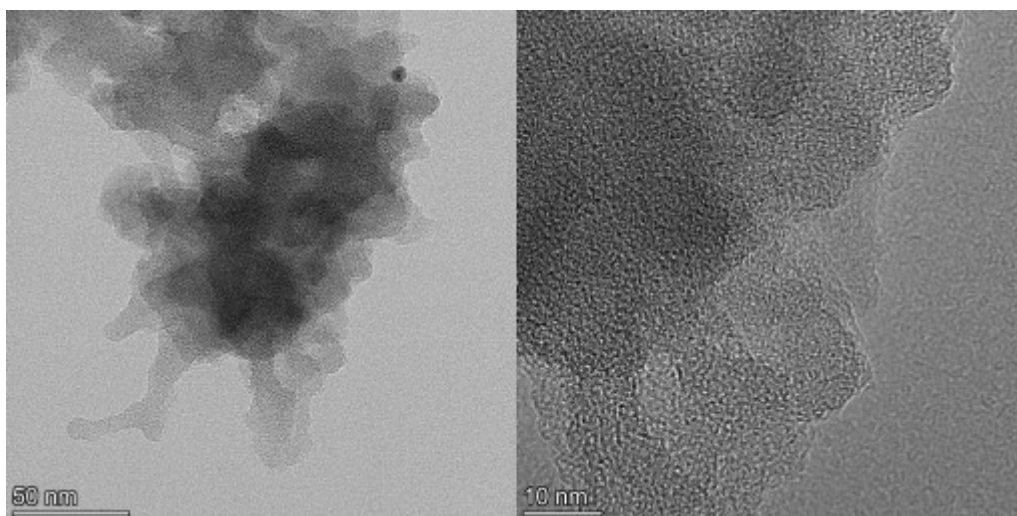


Figure S12. TEM image of TeTz-COF2

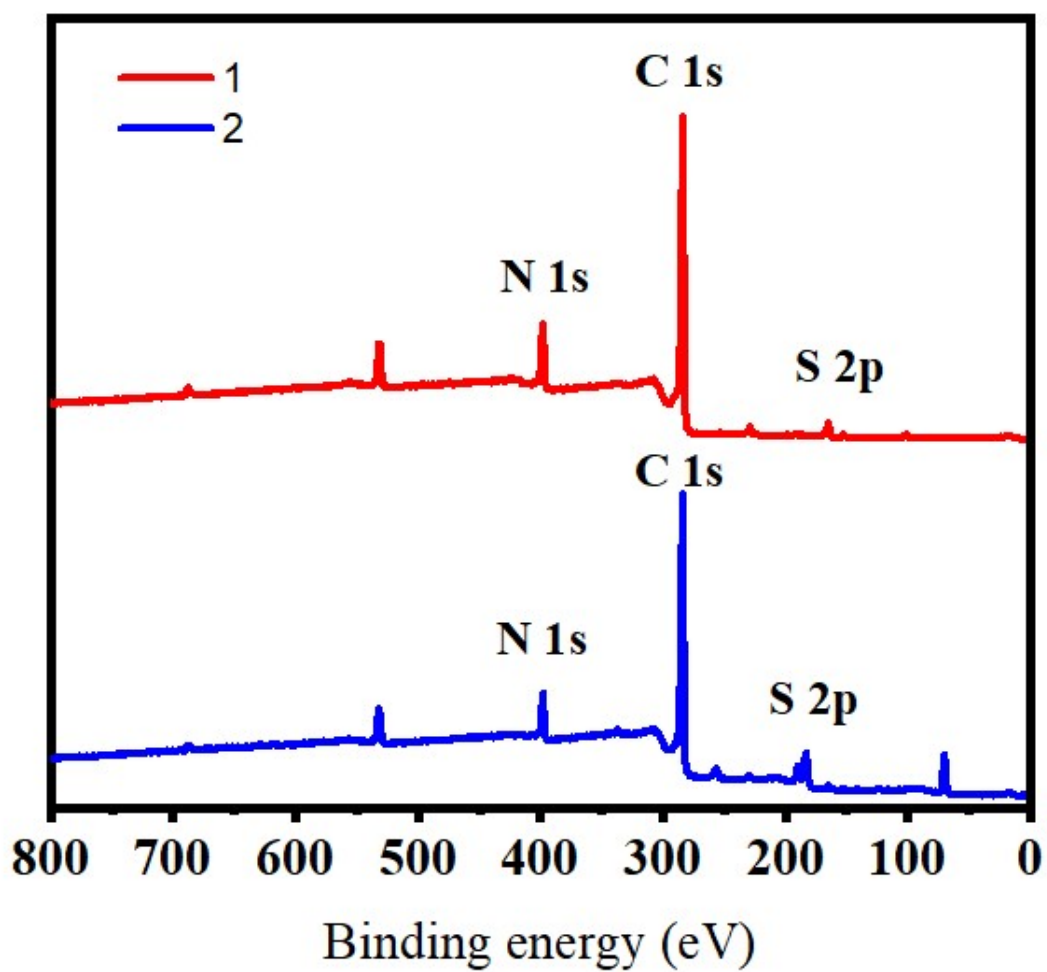


Figure S13. XPS survey spectrum of TeTz-COF1 and TeTz-COF2.

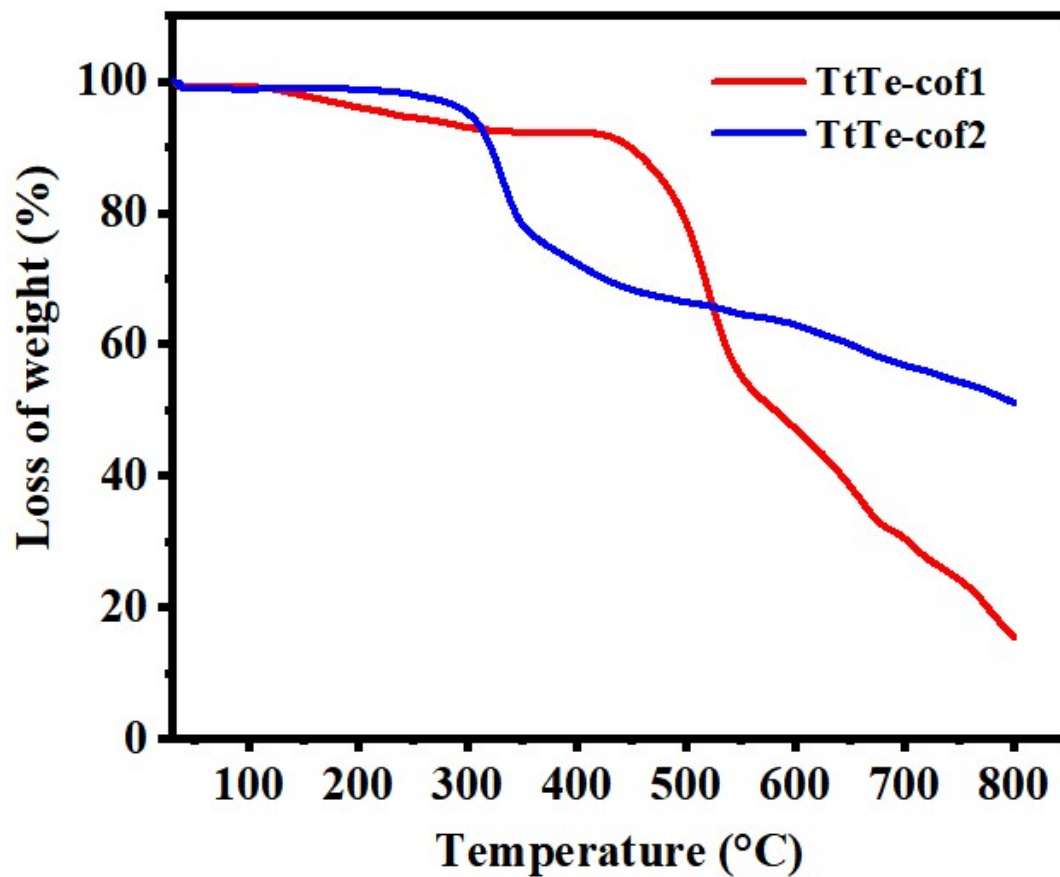


Figure S14. TGA data for TeTz-COF1 and TeTz-COF2.

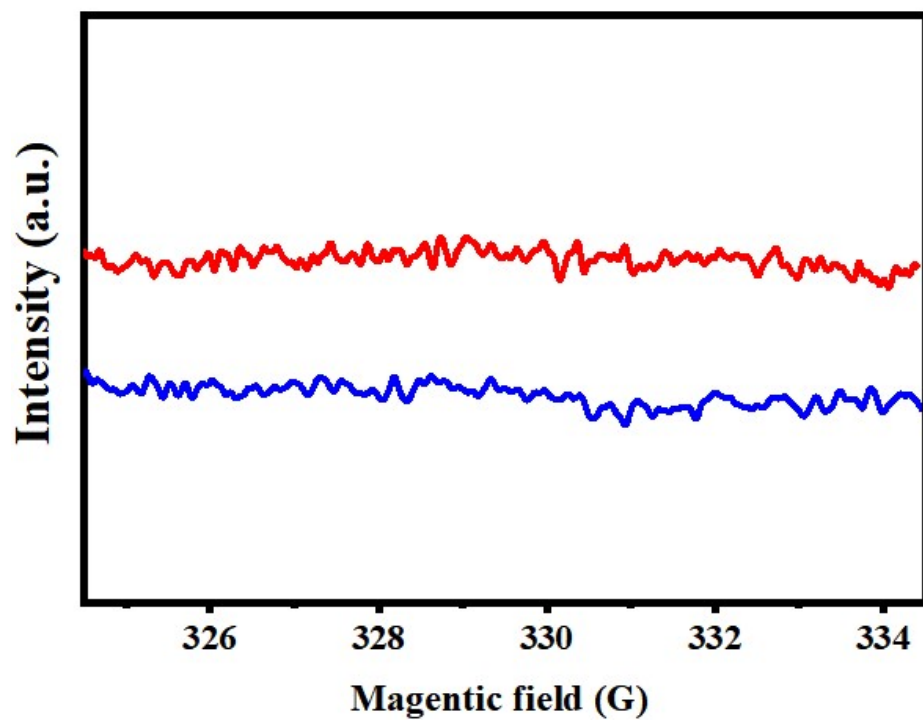


Figure S15. ESR spectrum of TeTz-COF1 and TeTz-COF2 in the darkness

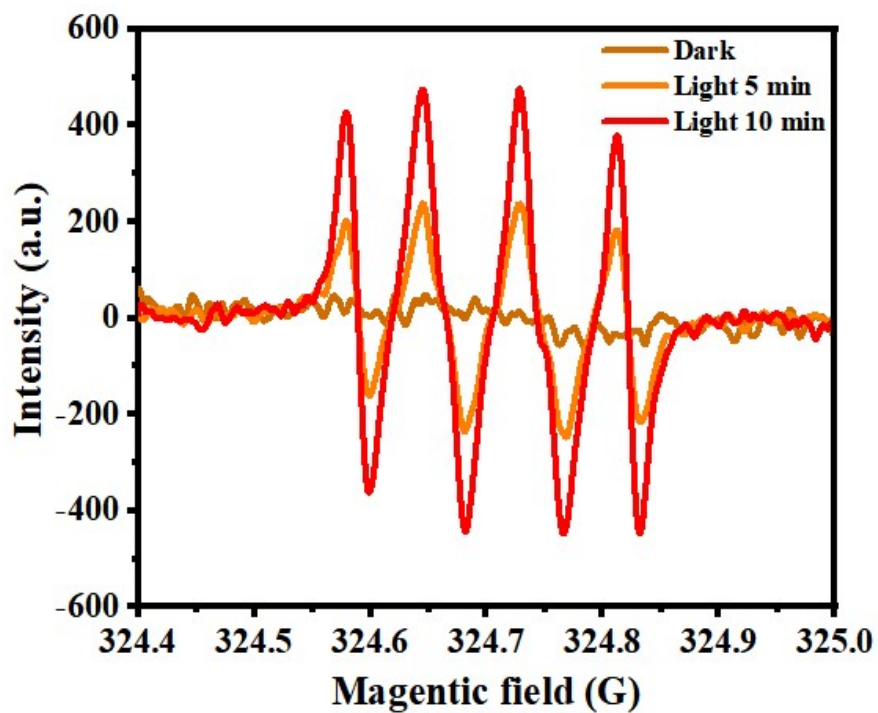


Figure S16. ESR spectra of TeTz-COF1

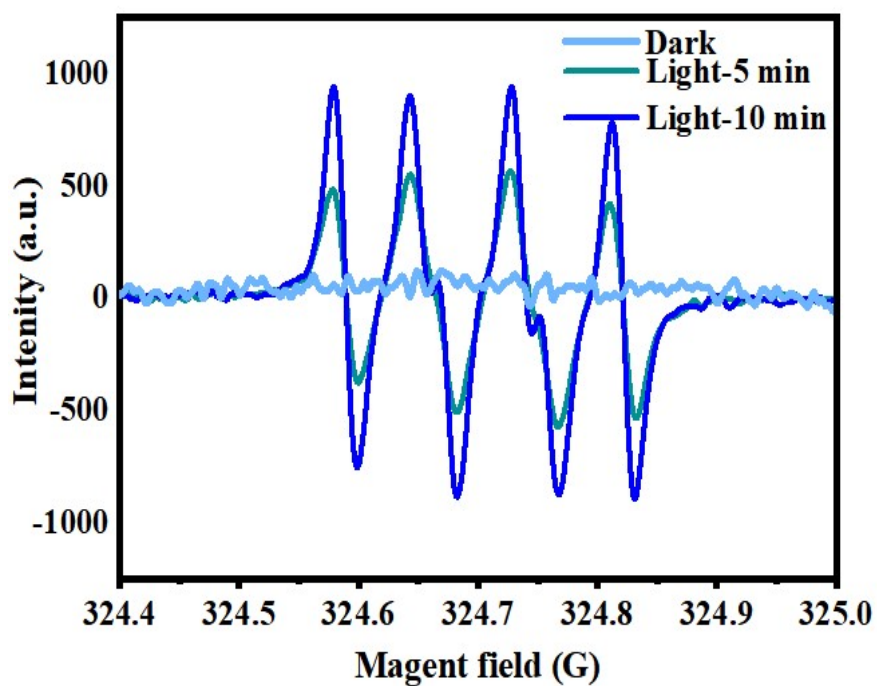


Figure S17. ESR spectra of TeTz-COF2

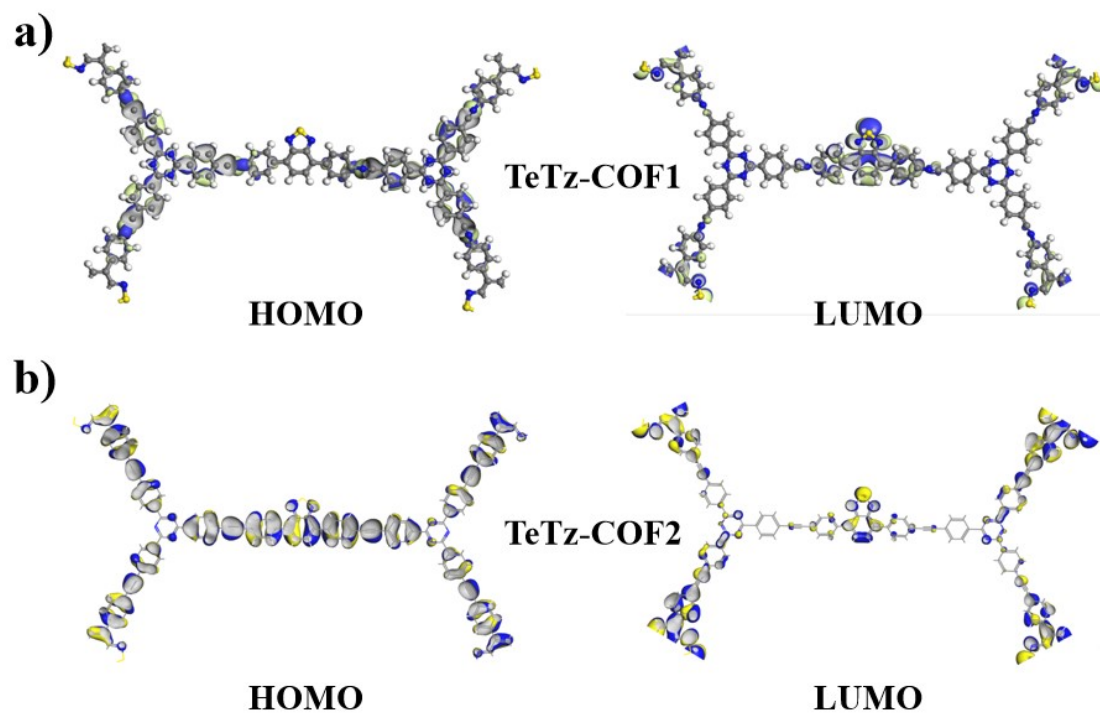


Figure S18. Frontier molecular orbitals and HOMO-LUMO energies of the smallest model unit of (a) TeTz-COF1

Table 1. Fractional atomic coordinates for the unit cell of sono TeTz-COF1.

Atom site label	Atom site type symbol	Atom site fract x	Atom site fract y	Atom site fract z	Atom site iso or equiv	U site adp type	Atom site occupancy
C1	C	0.34682	0.65012	-0.10432	0.00000	Uiso	1.00
N2	N	0.36316	0.68006	-0.10411	0.00000	Uiso	1.00
C3	C	0.36153	0.63210	-0.09815	0.00000	Uiso	1.00
C4	C	0.34562	0.60204	0.00013	0.00000	Uiso	1.00
C5	C	0.35966	0.58521	0.01418	0.00000	Uiso	1.00
C6	C	0.38970	0.59801	-0.07321	0.00000	Uiso	1.00
C7	C	0.40562	0.62791	-0.17549	0.00000	Uiso	1.00
C8	C	0.39169	0.64485	-0.18623	0.00000	Uiso	1.00
C9	C	0.40395	0.57983	-0.05025	0.00000	Uiso	1.00
N10	N	0.43121	0.58997	-0.14782	0.00000	Uiso	1.00
C11	C	0.49013	0.57007	-0.24952	0.00000	Uiso	1.00
C12	C	0.47463	0.58549	-0.26750	0.00000	Uiso	1.00
C13	C	0.44616	0.57329	-0.12385	0.00000	Uiso	1.00
C14	C	0.43322	0.54531	0.04178	0.00000	Uiso	1.00
C15	C	0.44899	0.53024	0.07089	0.00000	Uiso	1.00
N16	N	0.57032	0.54378	0.01341	0.00000	Uiso	1.00
C17	C	0.47781	0.54241	-0.07293	0.00000	Uiso	1.00
C18	C	0.54088	0.52575	0.01248	0.00000	Uiso	1.00
C19	C	0.49464	0.52622	-0.03612	0.00000	Uiso	1.00
C20	C	0.47957	0.49500	-0.02164	0.00000	Uiso	1.00
H21	H	0.32244	0.59175	0.07257	0.00000	Uiso	1.00
H22	H	0.34715	0.56221	0.09589	0.00000	Uiso	1.00
H23	H	0.42884	0.63808	-0.24575	0.00000	Uiso	1.00
H24	H	0.40437	0.66788	-0.26614	0.00000	Uiso	1.00
H25	H	0.51137	0.57962	-0.38455	0.00000	Uiso	1.00
H26	H	0.48444	0.60677	-0.40230	0.00000	Uiso	1.00
H27	H	0.41135	0.53562	0.15996	0.00000	Uiso	1.00
H28	H	0.43890	0.50956	0.21904	0.00000	Uiso	1.00
H29	H	0.45575	0.48224	-0.04650	0.00000	Uiso	1.00
S30	S	0.57983	0.57983	0.00000	0.00000	Uiso	1.00

Table 2. Fractional atomic coordinates for the unit cell of sono TeTz-COF2

Atom site label	Atom site type symbol	Atom site fract x	Atom site fract y	Atom site fract z	Atom site U iso or equiv	Atom site adp type	Atom site occupancy
C1	C	0.34811	0.65214	-0.21194	0.00000	Uiso	1.00
N2	N	0.36243	0.68134	-0.21176	0.00000	Uiso	1.00
C3	C	0.36423	0.63628	-0.20642	0.00000	Uiso	1.00
C4	C	0.34976	0.60619	-0.25455	0.00000	Uiso	1.00
C5	C	0.36492	0.59124	-0.24394	0.00000	Uiso	1.00
C6	C	0.39468	0.60610	-0.18431	0.00000	Uiso	1.00
C7	C	0.40931	0.63600	-0.13750	0.00000	Uiso	1.00
C8	C	0.39422	0.65103	-0.14909	0.00000	Uiso	1.00
C9	C	0.41017	0.59065	-0.16708	0.00000	Uiso	1.00
C10	C	0.42318	0.57773	-0.15050	0.00000	Uiso	1.00
C11	C	0.48161	0.55944	-0.25304	0.00000	Uiso	1.00
C12	C	0.46648	0.57440	-0.27346	0.00000	Uiso	1.00
C13	C	0.43873	0.56235	-0.12846	0.00000	Uiso	1.00
C14	C	0.42613	0.53530	0.03827	0.00000	Uiso	1.00
C15	C	0.44151	0.52065	0.06894	0.00000	Uiso	1.00
N16	N	0.55971	0.53387	0.01438	0.00000	Uiso	1.00
C17	C	0.46961	0.53251	-0.07493	0.00000	Uiso	1.00
C18	C	0.53105	0.51631	0.01299	0.00000	Uiso	1.00
C19	C	0.48601	0.51676	-0.03707	0.00000	Uiso	1.00
C20	C	0.47133	0.48635	-0.02208	0.00000	Uiso	1.00
H21	H	0.32672	0.59430	-0.30129	0.00000	Uiso	1.00
H22	H	0.35348	0.56809	-0.28150	0.00000	Uiso	1.00
H23	H	0.43234	0.64762	-0.08966	0.00000	Uiso	1.00
H24	H	0.40591	0.67415	-0.10908	0.00000	Uiso	1.00
H25	H	0.50230	0.56871	-0.38819	0.00000	Uiso	1.00
H26	H	0.47614	0.59507	-0.41078	0.00000	Uiso	1.00
H27	H	0.40473	0.52595	0.15492	0.00000	Uiso	1.00
H28	H	0.43168	0.50054	0.21800	0.00000	Uiso	1.00
H29	H	0.44813	0.47392	-0.04729	0.00000	Uiso	1.00
S30	S	0.56899	0.56899	0.00000	0.00000	Uiso	1.00

1. J. L. Shi, R. Chen, H. Hao, C. Wang and X. Lang, *Angew Chem Int Ed Engl*, 2020, **59**, 9088-9093.
2. J. Xu, C. Yang, S. Bi, W. Wang, Y. He, D. Wu, Q. Liang, X. Wang and F. Zhang, *Angew Chem Int Ed Engl*, 2020, **59**, 23845-23853.
3. I. Accelrys_Software_Inc, *Journal*, 2011.
4. Z. Ma, R. Sa, Q. Li and K. J. P. C. C. P. Wu, 2016, **18**, 1050-1058.